Role of Interfaces in Elasticity and Failure of Clay–Organic Nanocomposites: Toughening upon Interface Weakening?

György Hantal, Laurent Brochard, Roland J.-M. Pellenq, Franz-Joseph Ulm, Benoit Coasne

Role of Interfaces in Elasticity and Failure of Clay-Organic Nanocomposites: Toughening upon Interface Weakening?

György Hantal,[†,¶] Laurent Brochard,[‡,*] Roland J.-M. Pellenq,[†,⍰,§] Franz-Joseph Ulm,[†,§] and Benoit Coasne[†,§,#,*]

[†] Department of Civil and Environmental Engineering, Massachusetts Institute of Technology, 77 Massachusetts Avenue, Cambridge, MA 02139, United States

[‡] Université Paris-Est, Laboratoire Navier (UMR 8205), CNRS, ENPC, IFSTTAR, 77455 Marne-la-Vallée, France

[⍰] CINaM-CNRS, Campus de Luminy, 13288 Marseille cedex 09, France

[§] MultiScale Materials Science for Energy and Environment (MSE^2), joint CNRS-MIT Laboratory, 77 Massachusetts Avenue, Cambridge MA 02139, United States

* To whom correspondence should be sent. laurent.brochard@enpc.fr, benoit.coasne@ujf-grenoble.fr

Abstract. Synthetic organic-inorganic composites constitute a new class of engineering materials finding applications in an increasing range of fields. The interface between the constituting phases plays a pivotal role in the enhancement of mechanical properties. In exfoliated clay-organic nanocomposites, individual, high aspect ratio clay sheets are dispersed in the organic matrix providing large interfaces and hence efficient stress transfer. In this study, we aim at elucidating molecular-scale reinforcing mechanisms in a series of model clay-organic composite systems by means of reactive molecular simulations. In our models, two possible locations of failure initiation are present: one is the interlayer space of the clay platelet and the other one is the clay-organic interface. We systematically modify the cohesiveness of the interface and assess how the failure mechanism changes when the different model composites are subjected to a tensile test. Besides a change in the failure mechanism, an increase in the released energy at the interface (meaning an increased overall toughness) are observed upon weakening the interface by bond removal. We propose a theoretical analysis of these results by considering a cohesive law that captures the effect of the interface on the composite mechanics. We suggest an atomistic interpretation of this cohesive law, in particular, how it relates to the degree of bonding at the interface. In a broader perspective, this work sheds light on the importance of the orthogonal behavior of interfaces for nanocomposites.

INTRODUCTION

Organic-inorganic composite materials have attracted significant attention in recent years.[1] Among such hybrid materials, synthetic reinforced nanocomposites constitute a new class of structural materials with a wide range of promising applications in a number of fields.[2] Nature also produces a great variety of nanocomposites that often contain large amounts of mineralized components (e.g. 70% in bone or 95% in seashells). These natural nanocomposites can be characterized by enhanced strength, stiffness, toughness, and hardness at the same time. Their exceptional mechanical properties are the result of combining brittle inorganic inclusions of high yield stress and stiffness with a compliant low-density ductile organic material that provides cohesion upon large deformations.[3] These natural composite materials often have highly aligned reinforcing content which is organized in hierarchical structures. One of the most studied examples is nacre (also known as mother of pearl), found in mollusk shells, which is made up of brick-like aragonite platelets staggered in a protein/polysaccharide matrix.[4] A typical structural feature of natural nanocomposites is that inorganic inclusions have large aspect ratio (fibers or platelets) to provide large specific surface. The organic matrix, which is chemically bonded to these inclusions, facilitates stress transfer and provides additional means for energy dissipation under deformation. Depending on the nature of the interfacial bonding and the possible yield or fracture mechanisms at the interface, various toughening phenomena can arise upon failure.[5] Indeed, while the inorganic inclusion is mostly responsible for the composite strength and stiffness, it is the interface that provides toughness to the composite.

Of significant importance are organic-clay composite materials whose production in large quantities has recently become cheap thanks to improved fabrication techniques. Such materials are gaining popularity not only because of their remarkable mechanical properties

but also due to their low production costs. Depending on the degree of separation of the clay sheets three kinds of clay-organic composites can be distinguished: microcomposites, intercalated nanocomposites and exfoliated nanocomposites. In the first case, bigger clay particles in their preserved layered structure are embedded in the organic matrix; in an intercalated composite, clay particles adapt a sandwich-like structure where polymeric chains are incorporated in the interlayer space; while in exfoliated composites, individual clay sheets are dispersed in the polymeric matrix. The preparation of such an exfoliated composite, nylon-6 was first reported in 1993 by a group of researchers at Toyota who achieved 49% increase in tensile strength, 146% improvement in heat distortion temperature and 103% enhancement in Young's modulus with respect the pure polymeric material.[6] It has been shown that besides mechanical properties, it is also possible to improve chemical resistance, flame retardancy as well as gas barrier properties.

The reinforcing effect is clearly bound to the type of bonding between the two phases, and, in particular, to the area of the created organic-inorganic interface. When full delamination of clay sheets is achieved, the area of the interface can be of the order of several hundreds m^2/g. As a consequence, typically a small amount (cca. 5 wt%) of clay filler is sufficient to bring about substantial reinforcing effects.[7] Not only are these clay-organic composites cheaper to produce but they also seem to outperform fiber reinforced composites, which renders them one of the most competitive nanocomposite in the low filler content regime.[8] The number and type of bonds at the organic-inorganic interface play a vital role in attaining high mechanical performance. Indeed, individual clay platelets not only have to be dispersed but also integrated to a high degree in the polymeric matrix. However, the two components are often chemically incompatible, which can be improved by increasing either the organophyilic character of clay platelets or the hydrophyilicity of the matrix. Despite the increasing range of

applications of organic-clay composites there is still a pressing need to understand the mechanism of enhancement effects. Molecular simulation techniques provide a unique tool to investigate the different failure mechanisms at the atomic scale. Such an atomistic approach is needed when reorganizations in molecular bonding and structure are involved in failure mechanisms which control the macroscopic behavior of the material. In this context, we have already investigated the mechanical properties of crystalline silica, an amorphous carbonaceous material, and their interface by means of molecular simulation.[9] In another recent simulation study, the elastic and failure properties of illite, one of the most typical clay minerals, were also investigated.[10]

In this paper, our goal is to understand how the interface in a hybrid clay-organic system influences the elastic and failure properties of the composite as the degree of bonding at the interface is varied. Throughout this study we apply a reactive molecular force field to account for changes and reorganizations in the atomic structure when the system is mechanically loaded. The clay phase in the studied system consists of two stacked layers while the organic phase is modelled with a high-density disordered carbonaceous material with very low H and no heteroatom content. Such a model represents an almost fully exfoliated clay-organic nanocomposite. The system was created by cutting the bulk carbon into two halves which were then put in direct contact with the clay phase. Having free valences at the interface between the two phases has the above-mentioned activation effect that is often needed when the chemical character of the two phases is different. Bond formation and the relaxation of the so-created system is achieved in a simulated annealing scheme. Failure mechanisms in a tensile test are investigated when interface bonds are systematically removed. In fact, the studied system has the peculiar characteristic of having two possible locations of failure initiation: the clay-organic interface as well as the clay interlayer space in the platelet. We

observe two competing failure mechanisms depending on the cohesiveness of the interface. In the second part of this contribution we propose a theoretical analysis of these results. We identify a peculiar cohesive law to model the mechanics of the interface that captures the main features of the behavior of the composites. This cohesive law is consistent with a simple atomistic interpretation, which supports the physical validity of this analysis. Finally, we discuss the implication of this work in the field of mechanics of nanocomposite.

MATERIALS

Molecular models. The clay model used in this work was described in details elsewhere.[10] Here only the most important characteristics are summarized. Illite is the most common clay mineral in soils and one of the major clay constituents in argillaceous shale formations. The term illite is used to refer to a subgroup of minerals within the 2:1 dioctahedral phyllosilicate family.[11] The common characteristic of illite clays is that they are non-swelling aluminosilicates with exclusively potassium ions in the interlayer space. In what follows, we will use the term illite to refer to the typical composition based on the chemical formula given by Meunier and Velde, $K_{(x+y)}[Al_{(4-y)}Mg_y](Si_{(8-x)}Al_xO_{20})(OH)_4$.[12] Illite contains isomorphically substituted metal atoms in both the octahedral (O) and tetrahedral (T) layers as compared to the charge-neutral structure, pyrophyllite (chemical formula: $Al_4(Si_8O_{20})(OH)_4$). Illite differs from pyrophyllite in that about one Si(IV) atom per unit cell is replaced with Al(III) in a tetrahedral layer, and one Al(III) is substituted with Mg(II) (or sometimes Fe(II)) in the octahedral layer of about every second unit cell. Accordingly, we set $x = 1$ and $y = 0.5$ to have a net charge of -1.5e per unit cell as a result of the substitutions with metal atoms of lower valence. This is a typical layer charge of illite, which falls between that of micas (-2e) and smectites (-1e). However, while substitutions in mica and smectite occur mostly in the T and O layers, respectively, illite involves both kinds of substitutions. The negative charges

induced by the isomorphic substitutions in the layers are compensated with potassium ions. As a starting configuration, we use the pyrophyllite structure optimized by Refson et al. using high accuracy quantum chemistry calculations.[13] Isomorphic substitutions were then performed by ensuring that no oxygen atom has more than one substituted metal neighbor (*i.e.* the Loewenstein rule was respected). The initial structure is illustrated in Figure 1.

In this study, the organic phase was modelled with a high density amorphous carbon, the so-called CS1000 model which has a strong apolar character due to its void heteroatom content (the CS1000 structure is shown in Figure 1).[14] Indeed, CS1000 is a model of pyrolyzed saccharoze and, as such, represents a dense amorphous organic matrix.

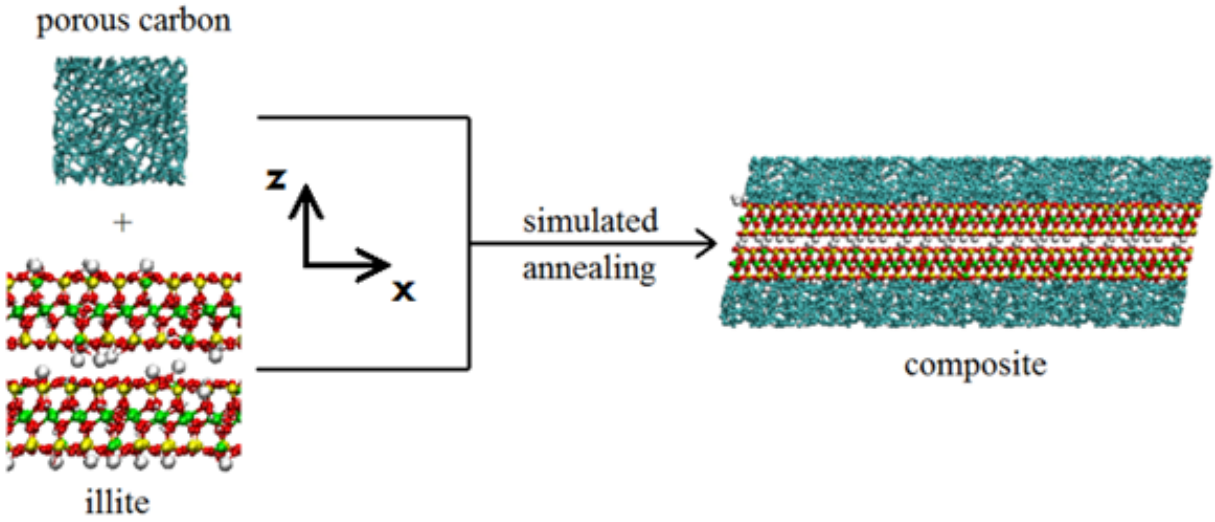

Figure 1. (color online) Hybrid organic-inorganic material considered in this work. The composite is made up of illite clay and a disordered porous carbon. The grey, yellow, green, red, and white spheres correspond to the C, Si, Al, O, and K atoms, respectively.

Preparation of the composite system. The first composite system was prepared using the two above mentioned bulk molecular models; illite and CS1000 were put in direct contact

and chemical bonds were allowed to form between the two phases in a simulated annealing procedure (Figure 1). The preparation of the composite made of these two phases gives rise to some technical issues. One of these issues is related to the different unit cell shape of the two phases; CS1000 has a cubic box while illite is triclinic (quasi-monoclinic). To set up the interface, a match of the two cells needs to be attained which was done by applying a careful transformation procedure to CS1000 while keeping its structure and porosity. The details of this protocol can be found in the Supporting Information.

Once the desired shape is reached, bond formation is induced between the organic and the mineral phases. In our previous work, we found that the presence of silanol groups at the surface of quartz was necessary to observe bond formation between silica and organic molecules.[15] However, clay layers are much less reactive than hydrated silica since the former do not contain surface silanol groups. Indeed, clay surfaces resemble the surface of a dehydrated reconstructed alpha-quartz. For illite, we considered the most probable cleavage surface, (001), by simply cutting bulk illite between two clay layers. CS1000 was cut along one face of the simulation box in order to produce a very reactive surface with many unsatisfied valences. To facilitate bond formation at the interface, the two phases were put in direct contact followed by a simulated annealing procedure using a reactive forcefield (see below). Only atoms in a 5 Å thick layer at the interface (*i.e.*, protruding 2.5 Å deep in each phase) were allowed to move to ensure that the interface disorder does not propagate too deeply in the two phases. The annealing protocol was the same as that used in our previous study dedicated to the interface of kerogen/silica composites.[15] The simulated annealing started at 600 K and the temperature was decreased gradually by 50 K at every step (except for the last 4 steps where it was set to 50, 25, 10 and 5 K). Simulation at every step was performed for 2 ps using the time step of 0.1 fs for the numerical integration of the equations

of motion. After the simulated annealing, a short reactive MD simulation was performed in the *NpT* ensemble for 20 ps at a temperature of 300 K and a pressure of 1 atm to release all residual stresses. As one could intuitively expect, the formation of alumino and silano-esters between the organic matter and illite was observed. A distance-based bonding analysis was carried out which found that about 11% of the O atoms (both basal and apical) in the top and bottom tetrahedral layers participate in forming bonds that connect the two phases. For more information, the reader is advised to refer to the Supporting information. The system prepared using the procedure above is illustrated in Figure 1.

It should be noted that the chemistry of clay-organic interfaces between micron-sized grains is very difficult to study experimentally. Here it is not our intention to give a description of the complex chemistry between clay and organic matter (for more information on the formation of special types of organic-clay chemical bonds the reader is referred to an ab initio study in Ref. 16). Our goal is to create bonds between the two phases and, once bonding has been established, test the mechanical and failure properties of this model composite. Since the empirical reactive force field was not designed to describe bonding between clays and organic matter, the chemical picture provided can only be considered highly approximate.

Composites with various degrees of interface bonding. As the selected CS1000 surfaces are highly reactive in our simulations, the resulting composite exhibits a high degree of bonding at the interface. Starting from this system, we generate additional composites through removal of interface bonds. In so doing, we obtain a collection of composite systems with varying degrees of interface bonding ranging from weak to strong bondings that constitute the basis of our investigation of the mechanical properties of clay-organic composites. As stated above, rather than focusing on the particular interface chemistry, we

perform a parametric mechanical study that spans over the possible degrees of interface bonding.

To derive a collection of composite systems we randomly remove bonds from the original composite. A simple analysis based on the distance between certain atoms showed Si-O-C and Al-O-C links formed between the two phases (for more details, see Supporting Information). Each newly prepared structure is relaxed in a short (2 ps) simulation to let the interface readapt to the new degree of bonding. The removal of bonds is carried out by replacing the bonding C atom with a H atom. As the organic phase turns out to be very "sticky" (as it still contains unsatisfied free valences) and reform bonds to the mineral phase, the final number of interface bonds is always different from our target and hence bond removal had to be performed repeatedly to reach low enough bond numbers. Mean bond numbers are calculated for each system by averaging over the last 20 configurations of a sampled equilibrium simulation. Systems with the following percentage of average bond numbers with respect to the original system are considered: 89.8%, 68.8%, 63.0%, 50.2%, 37.0%, 33.1%, and 23.2%.

Details of the computer simulations. Molecular simulation of failure in a covalently bonded system requires a force field that is able to account for bond breaking and formation. In this study we choose one of the most widely used reactive molecular force fields, ReaxFF.[17,18] The parameter set was developed by Pitman and van Duin and was first applied to simulate water confined between smectite clay and zeolite.[18] As discussed in our previous work, we slightly modified the force field to include parameters for K ions.[10] Molecular interactions are cut off at 9.3 Å and, according to the original parameterization, no long-range correction is applied. Series of molecular dynamics simulations are carried out with the LAMMPS

program package in the canonical ensemble, i.e. stain-driven mechanical tests are performed.[19] The temperature of the simulation, T = 300 K, is maintained using a Nose-Hoover thermostat with a damping constant equal to 10 fs. The time step for the integration of equations of motion is 0.1 fs. At each strain, an energy minimization is performed prior to the molecular dynamics simulation. Simulation of each step is 10 ps long. The elements of the stress tensor ($\underline{\underline{\Sigma}}$) are calculated from the virial expression and averaged for every deformation step:

$$\Sigma_{\alpha\beta} = -\frac{1}{a_x b_y c_z}\langle\sum_{i=1}^{N}\frac{p_{i,\alpha}p_{i,\beta}}{m_i} + \sum_{i=1}^{N} r_{i\alpha} f_{i,\beta}\rangle \quad (1)$$

where **a**, **b**, and **c** denote the three box vectors while the subscripts *x*, *y*, and, *z* refer to vectorial components along the three directions in our Cartesian coordinate frame. α and β represent any of these components. The index i (= 1, ... , N) runs over all N atoms in the system. m_i, $\mathbf{p}_i$, and, $\mathbf{r}_i$ correspond to the mass, momentum, and position of atom i, respectively, while $\mathbf{f}_i$ is the force acting on it. Equilibrated configurations are sampled and saved for further analysis. Periodic boundary conditions are used in the three directions *x*, *y*, and *z*.

RESULTS AND DISCUSSION

Nanocomposite Failure. We present in this section the elastic and failure properties of the original nanocomposite (having the highest degree of bonding) when subjected to a tensile test. The tensile test considered is a uniaxial displacement loading in the direction orthogonal to the layering, while keeping the other dimensions of the system constant. The simulated stress-strain curve is presented in Figure 2, and compared to those of bulk illite and bulk CS1000.[9,10] We also display in Figure 2 a few snapshots of the molecular system along the tensile test. We found that the composite system is much more compliant than each of the

bulk phases. As in the case of illite and CS1000, the behavior is linear at small loadings but with a lower stiffness. At large loadings, the composite exhibits strain hardening, which is also the case for illite. However, the critical strain of the composite is significantly larger than that of illite. Finally, the composite system fails inside the illite phase at a stress comparable to the yield stress of bulk illite. Accordingly, for this first composite system, the high degree of bonding at the interface provides high strength between illite and CS1000, such that failure does not occur at the interface but inside a phase with a lower strength (illite). The failure is unstable for bulk illite: a crack is initiated and propagates immediately over the whole system. In contrast, the failure of the composite is stable: a crack is initiated in illite and its propagation is mostly stable under displacement control. This stability difference can be rationalized with the results of Karihaloo et al.[20] based on the geometry of the systems studied (Figure 1). More specifically, these authors concluded that fractures propagating unstably can become stable in more elongated systems (note that the simulation box of bulk illite is quite short but the geometry of the composite is elongated in the direction of the initiated crack; see Supporting Information). As opposed to bulk illite, the studied composite has a geometry that indeed fails in the domain of stability.[20] Note also that, although this analysis can give a qualitative picture on the stability of fracture propagation, it is based on linear elastic fracture mechanics under the assumption of small scale yielding, the applicability of which is of course questionable for such nanosystems. As for CS1000, its strength is one order of magnitude higher than that of illite and that of the composite. Therefore, on the one hand, no fracture propagation in CS1000 is expected and, on the other hand, the mechanical behavior of CS1000 can be considered linear elastic for all the loading conditions considered.

The energy released (which directly characterizes the toughness of the material) during the tensile test per unit area of crack created, or critical energy release rate G_c, is obtained by integrating the strain-stress curves:[9,10]

$$G_C = \frac{V}{A_{crack}} \int_{loading} \Sigma_{zz} \mathrm{d}E_{zz} \qquad (2)$$

where V is the volume of the system and Σ_{zz} and E_{zz} are, respectively, the stress and the strain in the zz direction, which is perpendicular to the layers, and where displacement is only prescribed and allowed. A_{crack} is the area of crack created (assumed here to be molecularly flat, i.e., $A_{crack} = L_x L_y$ with L_x and L_y the dimensions of system in the direction of the crack). According to Eq. 2 the critical energy release rate of illite is G_c = 0.48 J/m^2, while that for the composite is twice as large: G_c = 1.11 J/m^2. Note that this is an overestimation of G_c for illite since the crack propagation is unstable. Nevertheless, we found that the apparent energy released during the failure is much larger for the composite system than for illite, which is surprising since failure occurs in illite in both cases so that one would expect the same energy release.

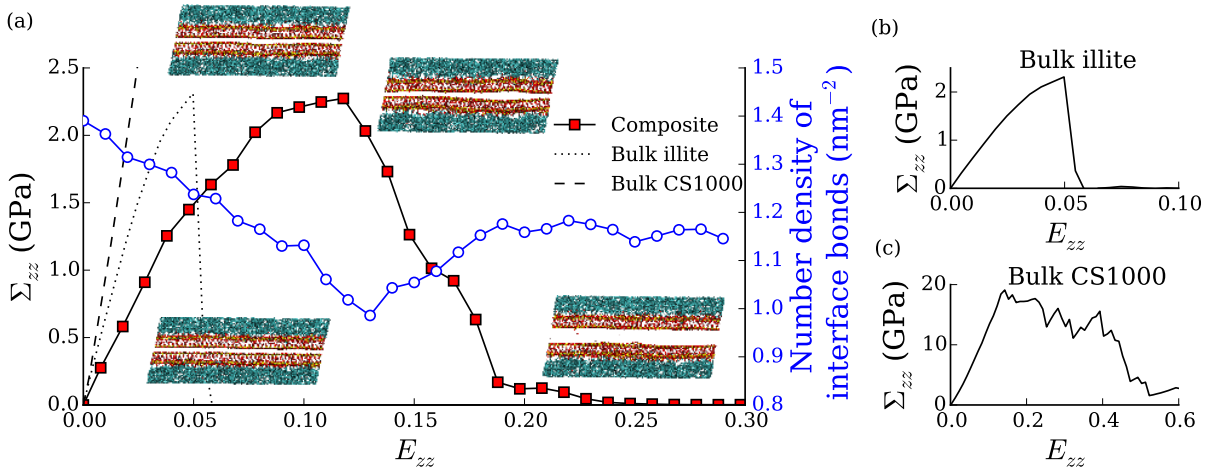

Figure 2. Stress-strain curves (Σ_{zz} vs. E_{zz}) of the composite system during the tensile test (when displacements only along the z direction, i.e. perpendicular to the clay layers, are applied and the corresponding zz stress is calculated) along with the number density of interface bonds (a). The behavior of bulk illite (b) and bulk CS1000 (c) are displayed on the

right panel for comparison. Interface bonds ((a) right axis) are getting broken upon loading, which provides additional source for energy release. Interface bonds are partially recovered after crack propagation in illite.

The apparent discrepancy between the critical energy release rates of illite and of the composite may be attributed to a partially irreversible degradation of the interface taking place concurrently with the failure in illite. This degradation is however insufficient to lead to failure at the interface. To confirm this hypothesis, we identified chemical bonds at the interface (see Supporting Information for details) and quantified their occurence in each strain step during the mechanical test. The surface density of bonds is presented in Figure 2a (see right vertical axis) as a function of the strain. This curve shows that the number of interface bonds indeed decreases up to the occurrence of a crack in illite, which corresponds to 29% of the bonds broken at this point. This is followed by a partial recovery of interface bonds with crack propagation and stress relaxation. At the end of the process, there are 16% fewer bonds than in the initial configuration. This result shows that the interface contributes significantly to energy dissipation upon failure of the composite, even if ultimately crack occurs in illite. Hence this interface degradation gives rise to a toughening of the composite with respect to pure illite. We note that the layered geometry considered here is very peculiar; in actual clay-organic composites, the contribution of interface degradation to the overall failure can differ from the case studied here.

Effect of Interface Strength. In an attempt to give a thorough description of the mechanical properties of clay-organic interfaces, we take our analysis one step further and study other composites derived from the original system after systematic removal of interface bonds. As discussed in Section 2.3, we considered 7 additional composite systems containing 89.8%,

68.8%, 63.0%, 50.2%, 37.0%, 33.1%, and 23.2% of the interface bonds present in the original composite system. In what follows, we will use these percentages to refer to the different composite systems.

First, a tensile test was performed for each composite system. The resulting stress-strain curves, plotted in Figure 3, can be divided into two groups. The first group, comprising the systems 89.8%, 68.8%, 63.0%, and 50.2%, displays failure inside the illite phase as in the original composite. The second group, which is composed of the systems 37.0%, 33.1%, and 23.2%, displays failure that occurs at the interface. To reduce the computational cost of the lengthening calculations of the mechanical test of the systems 33.1% and 23%, we applied larger strain steps (1.5% instead of 1%) to these systems, as well as a larger integration time step for the equations of motion (0.2 fs instead of 0.1). As shown in Figure 3, the lower the degree of bonding, the lower the composite strength. However, strain hardening is enhanced and failure occurs at larger strains. The decrease of the strength is somehow unexpected for the systems shown in Figure 3a; they all fail inside illite so that one could expect the stress at failure to be equal to the yield stress of illite. The reason for this is that the lower the degree of bonding at the interface, the more heterogeneous the distribution of stress in the system. As an example, we display in Figure 4a a few snapshots of the molecular system 50.2% along with its stress-strain curve. While for the original system the phases are almost uniformly stretched along the vertical direction (see Figure 2), the system 50.2% exhibits large inhomogeneity of the strains and thus stresses (see Figure 4). As a consequence, the local stress inside the illite phase can significantly exceed the average stress displayed in Figure 3 and Figure 4 (which explains why the strength of the composite can be lower than the strength of illite, even though failure occurs inside the illite phase). The strain and stress inhomogeneity in Figure 4 originates from the heterogeneity of the interface bonding; weak

interfacial areas tend to deform more than strong areas. The effect of interface heterogeneity becomes more important as there are fewer bonds at the interface, which explains why the strength of the composite decreases with the degree of bonding.

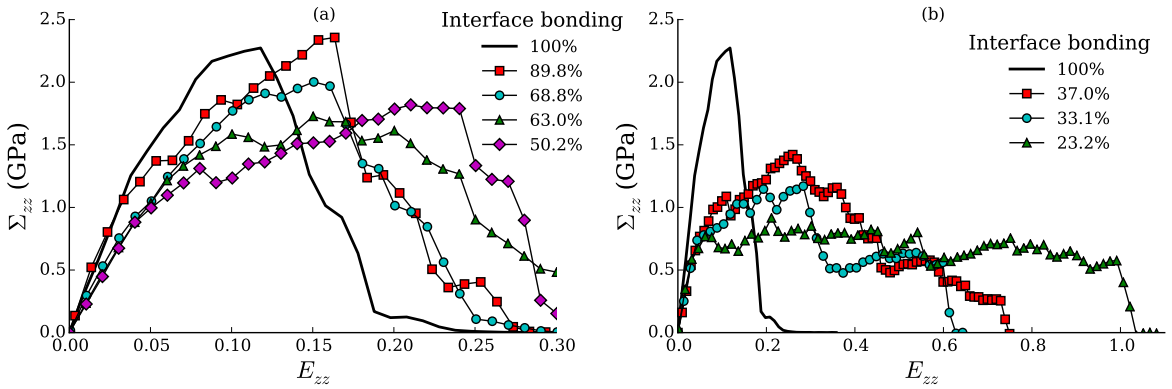

Figure 3. Tensile stress-strain curves computed for the original composite and systems with different degrees of interface bonding. Composites with an interface bond density higher or equal to 50.2% fail in illite (a), while composites with an interface density lower or equal to 37.0% exhibit failure at the interface (b).

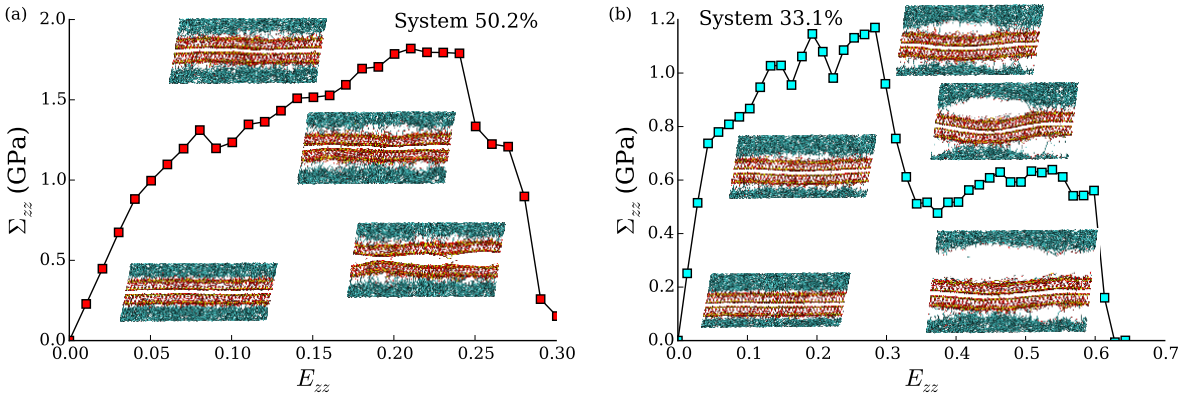

Figure 4. Stress-strain curves of systems 50.2% (a) and 33.1% (b) along with a few molecular configurations. These curves illustrate the two failure modes of the composites studied: failure in illite (a) or at the interface (b).

Figure 4 illustrates the irreversible degradation of the clay-organic interface during the tensile tests. A comparison of the stress-strain curves reveals that the strength of the interface in the system 50.2% is barely larger than the strength of illite as the failure appears very close to occurring at the interface. Table 1 summarizes the released energies in the composite systems computed using Eq. (2). We observe an increasing trend of the released energy as interface bonds are removed. The deviation from this trend observed for system 89.2% is attributed to anomalous bonding that appeared inside the interlayer space of illite due to some atypical local stresses arising during the tensile test (it also explains the unexpected large strength of this composite). The relationship between the degree of interface bonding and the interface degradation is not straightforward. This trend together with the change in the location of the crack propagation can be rationalized with the following scenario. Initially, as interface bonds are removed, the compliance of the interface increases and the system reaches larger strains. At the same time, the strength of the interface decreases leading to more broken bonds and consequently more released energy up to the failure in illite. As further bonds are removed, the interface becomes weaker than illite leading to the crack propagation occurring at the interface. However, this further decrease of interface bonding triggers an additional phenomenon resulting in an even larger compliance and thus additional mechanical energy release upon failure. This phenomenon is the consequence of the strain inhomogeneity along the interface which is directly related to the inhomogeneity of interface bonds; As bonds are removed, unevenness in bond density along the interface becomes more probable, in other words, the appearance of zones with fewer bonds and thus lower strength locally is expected. Due to their lower strength, these zones have a large probability to become even less populated with bonds. Upon this increasing inhomogeneity (as such a zone becomes wide enough) illite can adapt to this situation and further decrease the stress by adopting a bent, wavy shape. The adaptation of this wavy mode (illustrated in Figure 4b) is a way to further

decrease the stiffness, and increase the critical deformations that the composite can sustain. Triggering such a deformation provides an additional means of storing mechanical energy when the system is loaded, which contributes to the increase of fracture energy. This deformation can be characterized with an elasticity constant which controls the amount of mechanical energy stored by this deformation: the lower this elasticity constant, the higher the stored mechanical energy. Note that when calculating the energy released displayed in Table 1 (Eq. (2)), we considered the same crack surface area for the first series of systems (100%, 89.8%, 68.8%, 63.0%, 50.2%) and for the second series (37.0%, 33.1%, 23.2%) corresponding to a single crack propagating across the system. This choice is reasonable for the first series since these systems fail with one crack inside illite but is questionable for the second series since failure occurs at both interfaces. Therefore, direct comparison between the two series is not straightforward.

Table 1. Calculated released energies and failure location of the composites as a function of the degree of bonding at the interface.

Degree of interface bonding	Interface bond number density (nm^{-2})	Fracture energy, G_c (J/m^2)	Failure location
100%	1.39	1.11	illite
89.8%	1.25	1.42	illite
68.8%	0.96	1.27	illite
63.0%	0.87	1.44	illite
50.2%	0.70	1.54	illite
37.0%	0.51	1.95	interface
33.1%	0.46	1.87	interface
23.2%	0.32	2.85	interface
Bulk illite		0.48	-

Interface Opening and Cohesive Stress. As seen in the previous section, the clay-organic composites exhibit high compliance, large strain hardening and large energy release, which cannot be explained by the sole behavior of the clay and organic phases. Understanding the

mechanics of the interface is essential to explain those anomalous properties. In this section, we analyze the contribution of the interface to the mechanics of the composites and propose a mechanical model, based on a cohesive law, that captures the behavior of the interface.

Let us start by considering the original composite system ('100%'). As shown in Figure 2, the composite is significantly more compliant than each of the bulk phases. This excessive compliance cannot be explained by a peculiar deformation mode (such as that observed in Figure 4b) since the typical molecular configurations in Figure 2 do not show strain inhomogeneity. Excess compliance appears even at low loadings for which the stress can be considered homogeneous through the different layers of the composite. A significant part of the deformation is therefore to be attributed to the interface.

If we assume the homogeneity of the stress (Σ_{zz}) in the composite system in a direction perpendicular to the layers, the strain of illite (E_{illite}) and CS1000 (E_{CS1000}) are approximated as $E_{illite} = \Sigma_{zz} / K_{illite}$ and $E_{CS1000} = \Sigma_{zz} / K_{CS1000}$, respectively. The elasticities of bulk illite and CS1000 for the range of stresses and strains considered here are K_{illite} = 62 GPa and K_{CS1000} = 100 GPa which we estimate from the initial slope of the stress-strain curves of the bulk materials (see Figure 2) to keep the discussion simple. Therefore, one can easily evaluate what part of the composite deformation should be attributed to the interface:

$$L_z E_{zz} = L_z^{illite} E_{illite} + L_z^{\mathrm{CS1000}} E_{CS1000} + 2\delta_{interface} \quad (3)$$

where $\delta_{interface}$ stands for the apparent opening of one interface, while L_z^{illite} and L_z^{CS1000} denote the thickness of the two phases. $\delta_{interface}$ is multiplied by 2 in Eq. (3) since the system contains 2 interfaces. The general purpose of a 'cohesive law' is to determine a relationship between the cohesive stress acting on the interface (which is equal to Σ_{zz} due to the mechanical equilibrium of the system) and its opening $\delta_{interface}$. Such a $\Sigma_{cohesive} =$

$f(\delta_{interface})$ relationship characterizes the mechanics of the interface and provides valuable insight into the failure mechanism if material properties and geometries are properly taken into account. Figure 5 displays the contribution of the interface (determined simply by subtracting the weighed contribution of the two phases from the total stress-strain curve, see Eq. (3)) to the deformation of composite 100% until the onset of failure. It appears that the interface contributes to most of the deformation, from about 50% at low loadings to 75% at large loadings. The relationship between the interface opening and the cohesive stress across, which is significantly non-linear, can be accurately fitted by an exponential law.

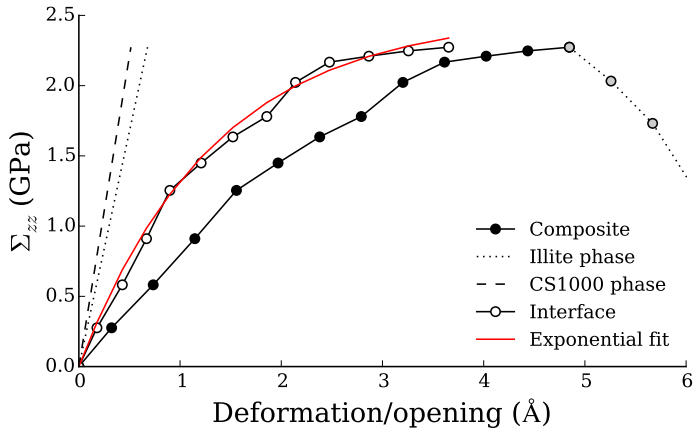

Figure 5. Contribution of the illite phase, the CS1000 phase, and the interface to the total deformation of the initial composite. Note the vertical axis showing now deformation instead of strain.

Our interpretation of the mechanics of the clay-organic interface is that the atomic structure of the bulk materials is strongly modified close to the interface, which gives rise to surface effects. A well-known surface effect is surface stress, often referred to as surface tension, which is a two-dimensional tension or compression tangent to the interface. However, the phenomenon observed here is orthogonal to the interface and corresponds to an apparent opening of the interface. The cohesive stress does not depend linearly on the opening; such a

non-linear behavior can be attributed to the breaking of interface bonds even at low loadings (see Figure 2). Each bond breaking softens the interface which becomes more compliant. In addition, bond breaking is at least partly irreversible as shown in Figure 2. Accordingly, the cohesive law is partly irreversible and the interface dissipates energy when loaded. This result explains the large released energies of the composite systems when compared to bulk illite.

Unique interface cohesive law. In this section, we propose a model of cohesive law for the interface that accounts for the density of interface bonds. As explained in the previous section, the relation between cohesive stress and interface opening can be well fitted by an exponential law. On the other hand, an exponential law is not a valid cohesive law since any cohesive law must converge to 0 at infinity (i.e., at large openings, the interface no longer transfers stress). Consequently, the exponential law describes the cohesive law up to moderate openings. As already mentioned, the non-linearity of this law is due to the breaking of interface bonds, which seems to depend linearly on the interface opening (Figure 2). Let us assume the following simple representation of the interfacial mechanics; the cohesive law of the interface is the superposition of the contribution of all the interface bonds, all assumed to be independent from each other. We also assume that these bonds have the same linear force-opening law (i.e. the exerted force can be characterized with the same mathematical expression as a function of the bond stretching), however they break at different critical openings (specific to each bond). In addition, if we also assume that the critical opening has a uniform distribution between 0 and δ_0, we find that the number of bonds decreases linearly with the opening and the overall cohesive law is a quadratic function of the opening:

$$\Sigma_{zz} = \rho_0 K_0 \delta \left(1 - \frac{\delta}{\delta_0}\right) \quad (4)$$

where ρ_0 is the bond density of the undeformed interface and K_0 is a constant such that $\rho_0 K_0$ is the interface elasticity when all bonds are intact. Following this simple representation of

the interface, we obtain a non-linear quadratic law that depends linearly on the interface bond density. We could fit the interface deformation reasonably well with a quadratic law in Figure 5, but it appears that such a law is not adapted to fit all stress-strain curves of the composites with varying degrees of interface bonding. Alternatively, inspired by the exponential fit of Figure 5, we found that a hyperbolic cosine cohesive law provides a satisfying fit for all the composites. The expression of the hyperbolic cosine law is as follows:

$$\Sigma_{zz} = \rho_0 \sigma_0 \left(1 - \frac{\cosh\left(K_0(\delta - \delta_{cr})\right)}{\cosh(K_0 \delta_{cr})}\right) \quad (5)$$

where σ_0 is a constant characterizing the yield stress of the interface per unit bond density, δ_{cr} is the interface opening for which the cohesive law is maximum, and K_0 is a constant characterizing the elasticity of the intact interface. The shape of the hyperbolic cosine differs a little from the shape of a quadratic law (see Figure 6) and captures well the behaviors of the various composites studied in this work. The simple approach that leads to the quadratic law is certainly too simple to capture the true behavior of the clay-organic interface. We display in Figure 6 (bottom right) the cohesive law for the different composites. The fitted values of the three parameters of the hyperbolic cosine cohesive law are: $\sigma_0 = 3.01$ GPa.nm^2, $\delta_{cr} = 4.83$ Å, and $K_0 = 0.60$ Å^{-1}. Figure 6 compares for each composite the tensile test strain-stress curves obtained by molecular simulation (black dot curves) to that predicted with the cohesive law assuming, for now, homogeneity of the stress (red curves):

$$L_z E_{zz} = \left(\frac{L_z^{illite}}{K_{illite}} + \frac{L_z^{CS1000}}{K_{illite}}\right) \Sigma_{zz}(\delta) + 2\delta \quad (6)$$

Figure 6 shows that this simple mechanical model based on the hyperbolic cosine cohesive law captures reasonably well the tensile tests up to failure in illite (after failure in illite, simulations curves are displayed with grey dots). On the other hand, the model fails to predict the behaviors of the systems with low degrees of bonding (33.1% and 23.2%) at large strains, because the stress homogeneity assumption does not hold for those systems (as will be

discussed and modeled in the next section). Otherwise, the predicting ability of the mechanical model is remarkable considering that only three parameters were fitted (σ_0, δ_{cr} and K_0) and the composite systems differ only in the initial interface bond density (ρ_0). Since this model is well adapted to describe failure at the interface, interface opening in systems where the composite fails eventually in illite can be well characterized at low deformations, up to the onset of failure in illite. Interface strengths as well as strain hardening (i.e. the changing slope of the stress-strain curves) are also well captured as the degree of bonding changes at the interface.

One could get more accurate fits by considering specific cohesive laws for each composite, but a single cohesive law is more valuable in the perspective of a physical analysis. The cohesive law provides a simple yet realistic understanding of the mechanics of the interfaces and provides the following conclusions on the failure mechanisms of such model organic-inorganic composites: (1) The interface contributes significantly to the overall deformation of the nanosystems with apparent openings going up to about 1 nm ($2\delta_{cr} = 9.66$ Å). (2) The strength $\rho_0\sigma_0$ and the energy release rate $\int_0^{2\delta_{cr}} \Sigma_{zz}(\delta)d\delta \propto \rho_0\sigma_0$ of the interface depend linearly on the density of interface bonds. (3) The mechanics of the interface is irreversible even at low strains (characterized by the non-linear shape analogous to a quadratic law). One can easily anticipate if failure occurs inside illite or at the interface, by comparing the interface strength $\rho_0\sigma_0$ to the strength of illite (2.2 GPa); failure occurs in illite for $\rho_0 > 0.73$ nm^{-2}, i.e. for a degree of bonding of 52% or more. Composite 50.2% is very close to this threshold. This system finally fails inside illite very close to the strength of the interface (Figure 6) and one can observe partial decohesion of the interfaces at failure (Figure 4a).

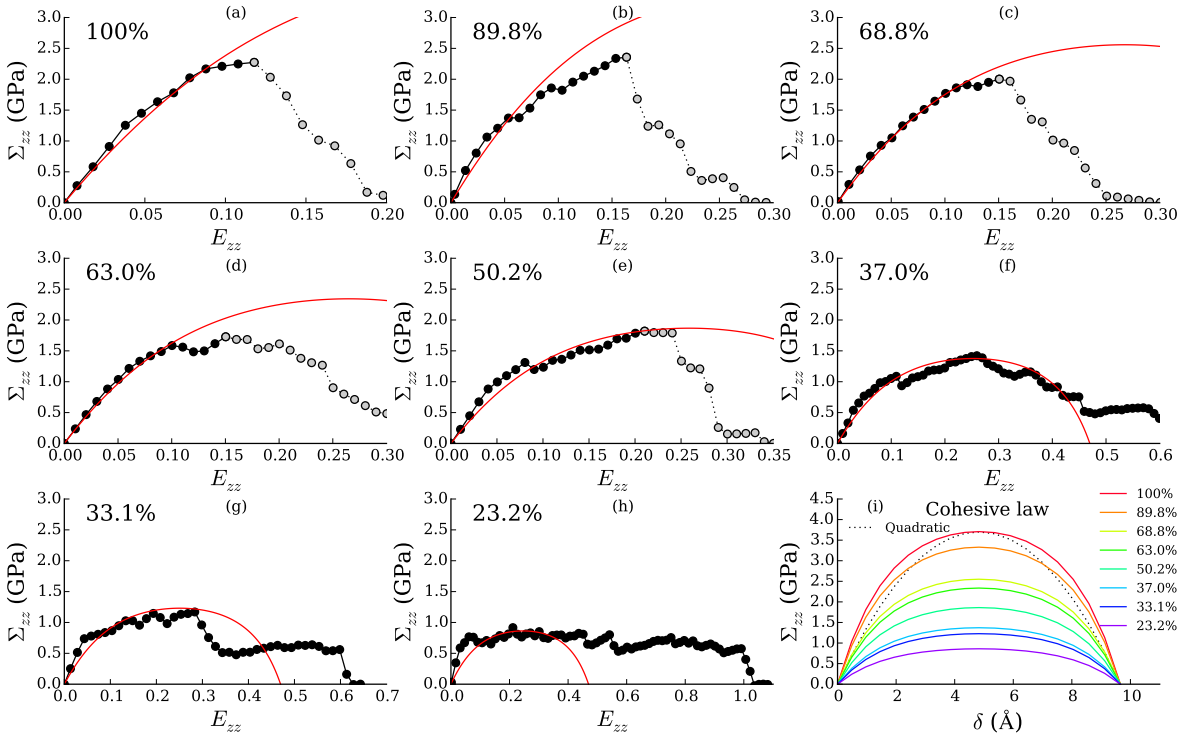

Figure 6. Tensile test strain-stress curves for the various composites, as obtained from molecular simulation (black dots) and from the cohesive law fitted to reproduce all curves with one single mechanical model assuming stress homogeneity (red line). The part of the curves represented with grey dots stand for the results of molecular simulation after the onset of the failure in illite, for which comparison between the model and the simulation results is irrelevant (since the cohesive law can predict failure at the interface only). The cohesive law representing the relationship between the cohesive stress and the opening of the interface is displayed at the bottom right (i). The shape of the hyperbolic cosine cohesive law is somewhat different from the quadratic law (dashed line) and it scales linearly with the degree of bonding at the interface (see text).

Accounting for interface heterogeneity. The major drawback of the mechanical model discussed in the previous section is the assumption that the stress is homogeneous in the nanocomposite. This assumption is convenient since the resulting mechanics of the system is

then very easy to interpret. However, it does not hold for large strains especially for composites with low degrees of bonding. Figure 4 shows that composite 33.1% adopts a wavy deformation mode at large strains. As discussed above this deformation mode originates from the non-uniformity of the strength along the interface, which causes debonding at weak points while stronger areas remain bonded. The wavy deformation mode can be observed for the three composites failing at the interface (23.2%, 33.1%, 37.0%) and, although only slightly pronounced, for some other composites before failure (composite 50.2% in particular). For the tensile tests, the consequence of the inhomogeneity is that the composite system is more compliant and can reach larger strains than expected following Eq. (6). This is particularly visible for composites 33.1% and 23.2% in Figure 6.

We developed a mechanical model of the composite system in which heterogeneities of the interface are accounted for. The detailed presentation and discussion of the model are available in the Supporting Information. The model is based on an analytical solution for an infinite plate loaded by even forces on its faces.[21] We applied this solution to the illite and CS1000 layers respectively, and, accounting for the various symmetries of the problem, we arrived at a self-consistent equation on the interface opening (Eq. (S9) in Supplementary Information). The problem can be solved numerically for any prescribed heterogeneous interface cohesive law. In particular, one can show that the wavy mode of deformation is indeed the consequence of the heterogeneity of the interface (Figure S3 in supplementary information).

We apply the approach developed to the three composites 37.0%, 33.1% and 23.2%. In each case, we seek for a way to characterize the interface heterogeneity that leads to a tensile test curve consistent with the molecular simulation results at large strains. The heterogeneity

could be introduced in the hyperbolic cohesive law in many different ways, but we restrain ourselves to do this through varying only the interface bond density ρ_0 in Eq. (5) as a function of the position along the interface. We display in Figure 7, for each of the composites 37.0%, 33.1%, and 23.2%, i) the simulated tensile test curves (black dots, right column), ii) the theoretical prediction based on the model assuming stress homogeneity presented in the previous section (red line, right column), iii) a possible interface bond density profile (blue curves, left column), and iv) the corresponding theoretical prediction accounting for the inhomogeneous distribution of interface bonds (blue curve right column). The purpose here is not to speculate about the nature of the interface heterogeneity since many types of heterogeneities can lead to the appropriate tensile test curves. The true heterogeneity of the interfaces may differ significantly from the representations proposed, e.g., imply varying the critical opening δ_{cr} or the non-universality of K_0. Nevertheless, our work proves that interface heterogeneity can explain accurately the mechanical behavior of the composites at large deformations. For the composite 37.0%, the improvement compared to the homogeneous model interface is limited since the prediction of the model assuming a homogeneous interface is already satisfying. In contrast, accounting for heterogeneity leads to much better results for the composites 33.1% and 23.2%. Note that the heterogeneity profile for the composite 23.2% contains a concentrated load, which enables to reach large deformations. As a consequence, this density profile leads to a higher average density than in the homogeneous case, and thus to a larger energy released. This adaptation was necessary since it is clearly apparent in Figure 7 that the energy released according to the molecular simulation exceeds significantly that predicted by the homogeneous model. The behavior of the composite 23.2% deviates from the linear scaling between bond density and amplitude of cohesive law. We attribute this discrepancy to the very low interface bond density (~ 0.3

bonds/nm^2), which may favor different chemical processes at the interface than for the other composites.

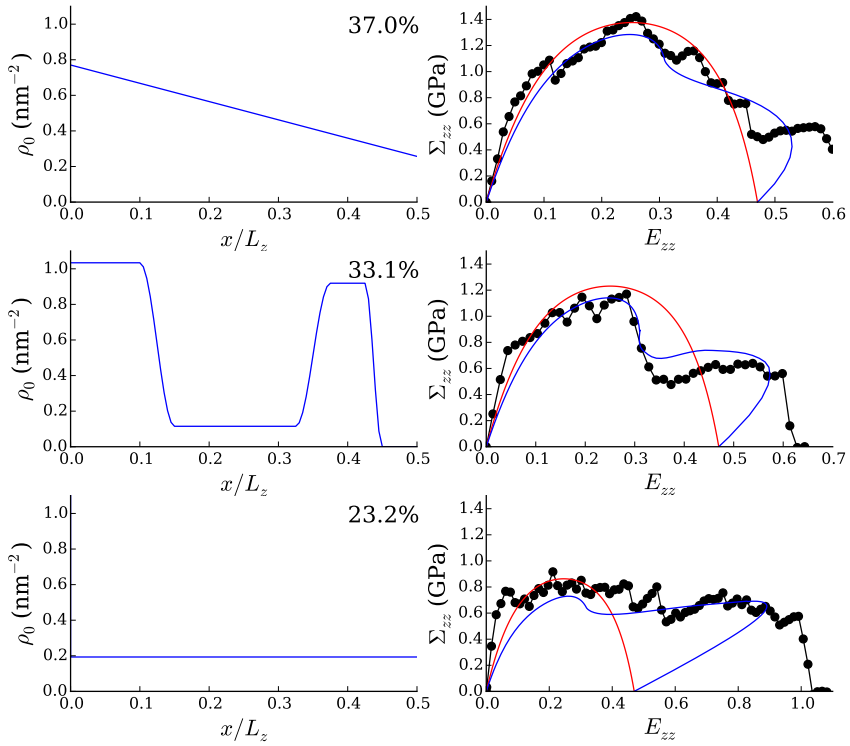

Figure 7. Possible interface bond density profiles for the three composites 37.0%, 33.1% and 23.2% (left), and the corresponding response to tensile test (blue curves, right) compared to the molecular simulation results (black dots, right) and to the homogeneous model (red curves, right).

General Relevance to Nanocomposites. In this work, we studied the mechanical and failure properties of a specific nanocomposite. However, our findings shed light on the importance of the orthogonal behavior of interfaces for the mechanics of nanocomposites. In the literature, a lot of effort has been dedicated to surface stresses (also known as surface tension), which is the mechanical effect tangent to interfaces.[22-24] In contrast, the phenomenon explored in this work is a mechanical effect orthogonal to interfaces. We described this orthogonal mechanical effect with a cohesive law which is a common description adopted for the mechanical behavior of materials at crack tips.[25] Interestingly, in

our work, the stress intercept of the cohesive law is zero, which means that the interface behavior affects not only the failure of the composite but also its elasticity at small loadings. For the examples studied in this work, the composites were 2 to 4 times more compliant than the bulk phases at small loadings, because of the effect of the interfaces. According to the cohesive law, the typical opening of the interface is about $2\delta_{cr}\sim 1$ nm, which means that this mechanical effect can affect only nanocomposites with heterogeneities with a size L that does not exceed a few tens of nanometers (the contribution of the interface to the total deformation is typically δ_{cr}/L). Such a phenomenon is totally relevant for exfoliated clay-organic nanocomposites where clay platelets have a thickness of around 1 nm.

The interface mechanics studied in this work has some interesting properties. First, the behavior of the clay-organic composites appears consistent with the magnitude of the interface cohesive law that scales linearly with the density of bonds. Consequently, the strength and the failure energy also scale linearly with the density of bonds. This intuitive scaling provides an easy way to characterize interfaces through the density of bonds. Second, the behavior of the composites is also consistent with a unique shape of the cohesive law (hyperbolic cosine) independent of the bond density. We discussed the physical origin of this shape (similarity with a quadratic law) and highlighted the fact that the non-linearity of this cohesive law is associated with irreversible bond breakings at the interface. The irreversibility of the interface mechanics is an essential finding of the present work. A consequence of such an irreversibility is that the composites release more energy during failure than illite, even if failure occurs inside the illite phase. Finally, at the nanometer scale, the interface cannot be viewed as perfectly uniform and we showed that interface heterogeneity is a key factor to explain the behavior of the composites with low interface bond densities. Those findings, which are valid for the clay-organic nanocomposites studied

here, raise interesting questions regarding the mechanics of nanocomposites in general. For instance, it suggests that the compliance, the strain hardening, and the critical energy release rate of nanocomposites may well exceed that of its constituents because of the interface opening and of the associated irreversible degradation of interfaces (even though ultimate failure occurs inside one of the bulk phases). It also suggests that the density of interface bonds and its heterogeneity are key physical properties that control quantitatively the interface mechanics.

SUMMARY AND CONCLUSIONS

We employed molecular simulation with a reactive molecular force field, ReaxFF, to investigate the mechanical and failure properties of a layered clay-organic nanocomposite. This hybrid system is composed of illite, one of the most common clay minerals in sedimentary rock formations as well as soils; and CS1000, a disordered porous carbon, which is used here to model the organic matrix. We submitted the composite to a tensile test orthogonal to the layering. Interestingly, the composite exhibited much larger compliance, strain hardening, and energy released at failure than the bulk phases (even though failure occurs inside the illite phase because of strong interface cohesion). By analyzing the interface bond density during the tensile test, we could explain this toughening with the breaking of interface bonds that provides an additional means for energy release.

We pursued this study by considering additional clay-organic nanocomposites with varying degrees of interface bonding. Starting from the initial composite, interface bonds were systematically removed and the tensile test was repeated. We found that the compliance and strain hardening increase with decreasing the interface bond density. Composites with a low

interface bond density were found to fail at the interface with a strength that seems correlated to the bond density. Surprisingly, the contribution of the interface degradation to the energy release appears to increase when decreasing the bond density. This result is quite counterintuitive since it shows that toughening is achieved by weakening the interface. Finally, further decrease of interface bonding leads to high inhomogeneity in the distribution of interface bond density which triggers a peculiar wavy deformation of the layers in the system thus further increasing the compliance and the stored mechanical energy upon failure.

We also analyzed these results by studying the mechanics of the composites in depth. In a first approach, assuming interface homogeneity, we found that a peculiar yet simple cohesive law representing the interface mechanics captures most of the properties of the composites: compliance, strain hardening, and failure location. The same cohesive law, which captures the behavior of all the composites regardless of the degree of interface bonding, relies on three parameters only. Discrepancy with molecular simulation results at large strains could be resolved by introducing interface heterogeneity in a second, refined mechanical approach. Heterogeneity triggers a wavy mode of deformation of the system which strongly affects the mechanical response to tensile test at large strains. In the light of this mechanical analysis, the unusual properties of the composites could be accurately described with the cohesive law, in which the key parameters that characterize the interface are the bond density and its heterogeneity. Although these results were obtained for a specific, nanoscopically layered clay-organic composite system, they shed light, in a more general context, on the importance of the orthogonal response of interfaces in the mechanics of nanocomposites.

Supporting Information

Description of some of the molecular simulation procedures and mechanical model accounting for interface heterogeneity. This material is available free of charge via the Internet at http://pubs.acs.org.

Present Addresses

¶Dept. of Computational Physics, University of Vienna, Sensengasse 8/9 1090 Wien, Austria

⁴Laboratoire Interdisciplinaire de Physique, CNRS and Université Grenoble Alpes, UMR CNRS 5588, 38000 Grenoble, France

Acknowledgements

This work was supported by the X-Shale project enabled through MIT's Energy Initiative in collaboration with Shell and Schlumberger. Additional support was provided by the ICoME2 Labex (ANR-11-LABX-0053) and the A*MIDEX projects (ANR-11-IDEX-0001-02) cofunded by the French programme ‘Investissements d'Avenir’ managed by ANR, the French National Research Agency.

References

(1) Ortiz, C.; Boyce, M. C. Bioinspired Structural Materials. *Science* **2008**, *319*, 1053-1054.

(2) Gomez-Romero, P.; Sanchez, C. E. *Functional Hybrid Materials*; Weinheim: Wiley, 2004.

(3) Smith, B. L.; Schäffer, T. E.; Viani, M.; Thompson, J. B.; Frederick, N. A.; Kindt, J.; Belcher, A. M.; Stucky, G. D.; Morse, D. E.; Hansma, P. K. Molecular mechanistic origin of the toughness of natural adhesives, fibres and composites. *Nature* **1999**, *399*, 761-763.

(4) Kamat, S.; Su, X.; Ballarini, R.; Heuer, A. H. Structural basis for the fracture toughness of the shell of the conch Strombus gigas. *Nature* **2000**, *405*, 1036-1040.

(5) Kim, J.-K.; Mai, J.-W. *Engineered interfaces in fiber reinforced composites*; UK: Elsevier Science Ltd., Oxford, 1998.

(6) Kojima, Y.; Usuki, A.; Kawasumi, M.; Okada, A.; Kurauchi, T.; Kamigaito, O. One-pot synthesis of nylon 6–clay hybrid. *Journal of Polymer Science Part A: Polymer Chemistry*, **1993**, *31*, 1755-1758.

(7) Gao, F. Clay/polymer composites: the story. *Materials Today* **2004**, *7*, 50-55.

(8) Fornes, T. D.; Paul, D. R. Modeling properties of nylon 6/clay nanocomposites using composite theories. *Polymer* **2003**, *44*, 4993-5013.

(9) Brochard, L.; Hantal, G.; Laubie, H.; Ulm, F.-J.; Pellenq R. J.-M. Fracture Mechanisms in Organic-Rich Shales: Role of Kerogen. *Poromechanics V*, 2471-2480.

(10) Hantal, G.; Brochard, L.; Laubie, H.; Ebrahimi, D.; Pellenq, R. J.-M.; Ulm, F.-J. ; Coasne, B. Atomic-scale modelling of elastic and failure properties of clays. *Molecular Physics* **2014**, *112*, 1294-1305

(11) Bergaya, F.; Then, B. K. G.**;** Lagaly, G. *Handbook of clay science*, 1st Ed. Elsevier: The Netherlands, 2006.

(12) Meunier, A.; Velde, B. *Illite. Origins, Evolution and Metamorphism*, Springer: Berlin, 2004.

(13) Refson, K.; Park, S. H.; Sposito, G. J. Ab Initio Computational Crystallography of 2:1 Clay Minerals: 1. Pyrophyllite-1Tc. *J. Phys. Chem. B* **2003**, *107*, 13376.

(14) Pikunic, J.; Clinard, C.; Cohaut, N.; Gubbins, K. E.; Guet, J.-M.; Pellenq, R. J.-M.; Rannou, I.; Rouzaud, J.-N. Structural Modeling of Porous Carbons: Constrained Reverse Monte Carlo Method. *Langmuir* **2003**, *19*, 8565-8582.

(15) Hantal, G.; Brochard, L.; Cordeiro, M. N. D. S.; Ulm, F.-J.; Pellenq, R. J.-M. Surface Chemistry and Atomic-Scale Reconstruction of Kerogen–Silica Composites. *J. Phys. Chem. C* **2014**, *118*, 2429-2438.

(16) Bocquet, M.-L.; Coasne, B.; Pellenq, R. J.-M.; Ulm, F.-J. Organic-Clay Interfacial Chemical Bonds Probed by ab Initio Calculations. *J. Chem. Phys. C*, **2015**, *119*, 6511-6517.

(17) van Duin, A. C. T.; Dasgupta, S.; Lorant, F.; Goddard, W. A. ReaxFF: A Reactive Force Field for Hydrocarbons. *J. Phys. Chem. A* **2001**, *105*, 9396-9409.

(18) Pitman, M. C.; van Duin, A. C. T. Dynamics of Confined Reactive Water in Smectite Clay–Zeolite Composites. *J. Am. Chem. Soc.* **2012**, *134*, 3042-3053.

(19) Plimpton, S. Fast Parallel Algorithms for Short-Range Molecular Dynamics. *J. Comput. Phys.* **1995**, *117*, 1-19.

(20) Karihaloo, B.L.; Wang, J.; Grzybowski, M. Doubly periodic arrays of bridged cracks and short fibre-reinforced cementitious composites. *Journal of the Mechanics and Physics of Solids*, **1996**, *44*, (10), 1565-1586.

(21) Sneddon, I. N. *Fourier Transforms*, McGraw-Hill Book Company: New York, 1951.

(22) Ibach, H. The role of surface stress in reconstruction, epitaxial growth and stabilization of mesoscopic structures. *Surface Science Reports*, **1997**, *29*, (5–6), 195-263.

(23) Müller, P.; Saúl, A. Elastic effects on surface physics. *Surface Science Reports*, **2004**, *54*,(5-8), 157-258.

(24) Dormieux, L.; Kondo, D.; Ulm, F.-J. *Microporomechanics*, Wiley: Chichester, 2006.

(25) Anderson, T. L. *Fracture mechanics: Fundamentals and Applications*, CRC Press: USA, 2005.

(26) Gelb, L. D.; Gubbins, K. E. Pore Size Distributions in Porous Glasses: A Computer Simulation Study. *Langmuir* **1999**, *15*, 305-308.

(27) Brenner, D. W.; Shenderova, O. A.; Harrison, J. A.; Stuart, S. J.; Ni, B.; Sinnott, S. B. A second-generation reactive empirical bond order (REBO) potential energy expression for hydrocarbons. *J. Phys.: Condens. Matter* **2002**, *14*, 783-802.

TOC Figure

Role of Interfaces in the Elasticity and Failure of Clay-Organic Nanocomposites: Toughening upon Interface Weakening?

György Hantal,[†,¶] Laurent Brochard,[‡,*] Roland J.-M. Pellenq,[†,∥,§] Franz-Joseph Ulm,[†,§] and Benoit Coasne[†,§,⊥,*]